



Modeling metal oxide nanoparticle GABA interactions: Complexation between the Keggin POM and γ -aminobutyric acid in the solid state and in solution influenced by additional ligands

Fredric G. Svensson, Philipp Simon, Vadim G. Kessler*

Department of Molecular Sciences, Swedish University of Agricultural Sciences, Box 7015, SE-75007 Uppsala, Sweden

ARTICLE INFO

Keywords:

POM
Metal oxide nanoparticle
Biomarker complex
GABA
Dopamine
Structure-directing agent

ABSTRACT

Phosphotungstic acid (POM) was crystallized together with the neurotransmitter γ -aminobutyric acid (GABA) in acidic medium to form [(HGABA)₃PW₁₂O₄₀], compound **1**. The latter would only crystallize in the presence of dopamine, while dopamine itself did not become a part of the complex, but crystallized separately as [(Hdopamine)₂HPW₁₂O₄₀], compound **2**, as previously reported. GABA interacts with POM via hydrogen bonding between the protonated amino group and a terminal oxygen on POM and also via protonated carboxylic acid group. Based on structural information from the crystal structures of **1** and **2** together with complementary studies using other catechols we attempted to provide molecular insight into the well-known structure-directing effect of dopamine. Strong hydrogen bonding between dopamine and POM, together with formation of “dopamine dimers” in the packed structure by interactions between the aromatic rings and intermolecular hydrogen bonding might be important factors for them in directing the self-assembly of polyoxometalates into complex hierarchical structures. Interaction between dopamine and GABA in solution was investigated by diffusion ordered spectrometry (DOSY) NMR in MilliQ-water and in 0.1 M HCl.

1. Introduction

Nanotechnology has potential to become a powerful tool within biotechnology and medicine [1–3]. Particularly the use of metal and metal oxide nanoparticles for bioimaging [4,5], drug delivery [6], wound healing [7,8], and plant protection [9] have gained increased interest. Still, the effects of nanomaterials on biological systems are far from well understood. The comparable sizes allow for interference with cellular components from nanomaterials. This is both a key feature in novel therapeutics based on nanomaterials but can also pose a health hazard for animals and plants alike [10,11]. Polyoxometalates (POMs) are polyatomic ions, usually oxo-anions (Mo, W, V, Nb, Ta), but sometimes also cationic ions (Al) with well-defined structure and composition and are often highly stable in solution [12,13]. They are usually classified as isopolyanions or heteropolyanions, where the former one consists of the same type of metal ions and the latter contains different metal/non-metal ions [14]. Several structural families have been described, including the Keggin, Lindqvist, Andersson, and Wells-Dawson structures [12]. The POMs can relatively easily be modified via metal substitution/modification [15,16] or organic functionalization

[17,18] and this offers great possibility to design new materials for a range of applications [14,19]. They have been reported to function as specific artificial peptidases by coordination between the POM and amino acid functional groups [20,21]. Proteins usually interact with POMs via electrostatic and/or hydrogen bonding and occasionally mediated via solvating water molecules [22]. Detailed insight into molecular interactions were obtained recently in the studies of Mo- and W-POM complexation with glycine-based oligo-peptides [23].

Antibacterial, antiviral, and antitumor effects have been well reported and are ascribed to interference between POMs and enzymes, inhibiting cellular processes [24,25]. The use of organic ligands, including biomolecules, to direct self-assembly of molecular components have been receiving increasing attention as a promising route to realize complex hierarchical structures via bottom-up process. These structurally complex assemblies may find applications in, for instance, drug delivery, adsorbents [26–29].

Several publications report the self-assembly of POMs and metal oxides into monodisperse flower-like aggregates using the neurotransmitter dopamine (a catecholamine) as structure-directing agent [28,30–32]. We recently reported the crystal structure of a

* Corresponding author.

E-mail address: Vadim.Kessler@slu.se (V.G. Kessler).

<https://doi.org/10.1016/j.ica.2021.120547>

Received 31 March 2021; Received in revised form 6 July 2021; Accepted 29 July 2021

Available online 31 July 2021

0020-1693/© 2021 The Author(s). Published by Elsevier B.V. This is an open access article under the CC BY license (<http://creativecommons.org/licenses/by/4.0/>).

Table 1
Crystallographic data for compound 1.

Chemical composition	C ₁₂ H ₃₀ N ₃ O ₄₆ PW ₁₂
Formula weight	3189.56
Crystal system	Rhombohedral
Space group	R-3
R1	0.0812
wR2	0.2418
Goof	1.005
a (Å)	18.303(16)
b (Å)	18.303(16)
c (Å)	24.50(2)
α (°)	90.00
β (°)	90.00
γ (°)	120.00
V (Å ³)	7107(11)
T (K)	296
Z	6
Nr. refl.	2544
θ min	2.23
θ max	25.25
Data completeness	0.996
CCDC reference	2074443

phosphotungstate-dopamine complex [33]. Crystal structures can give valuable insight into molecular interactions that result in the self-assembly processes and may provide guidance to discover new structure-directing ligands for novel self-assembly systems. Herein, we first report the crystal structure of another neurotransmitter of similar size to dopamine, γ -aminobutyric acid with phosphotungstate. We are interested in the biological effects of metal oxide nanoparticles and are seeking molecular models to better understand their influence on biological systems. The formation of [(HGABA)₃PW₁₂O₄₀], compound 1, is an example of the “cocktail effect” where the crystallization is dependent on the presence of dopamine, while dopamine itself does not make up part of the complex. This may be of relevance for understanding how nanoparticles are entering biological systems, e.g. via the gastrointestinal tract, and interact with a complex mixture of biomolecules in an acidic environment. Secondly, we used the structural models of compounds 1 and 2 in an attempt to obtain a better understanding of the factors contributing to the structure-directing effect of dopamine.

2. Materials and methods

Phosphotungstic acid hydrate (H₃PW₁₂O₄₀·H₂O, Sigma Aldrich, reagent grade), γ -aminobutyric acid (GABA, Aldrich, 99%), dopamine·HCl

(Aldrich), pyrocatechol (Sigma-Aldrich, >99%), 4-methylcatechol (Aldrich, > 95%), and 4-*tert*-butylcatechol (Aldrich, >98 %) were used as received. 1 M HCl was diluted from 37 % HCl (Aldrich). H₃PW₁₂O₄₀ was reacted with GABA and dopamine in a 2: 2: 1 M ratio in 1 M HCl. GABA and dopamine were dissolved first with the subsequent addition of the POM. This immediately resulted in a dark red, but transparent, reaction mixture. Crystals of compound 1 formed over night as red cubic crystals of about 1 mm formed overnight at room temperature. The crystals suffered from extensive twinning and crystals had to be cut manually to obtain a piece with single-domain orientation suitable for data collection. For powder diffraction analysis, the precipitates were washed three times with deionized water followed by centrifugation between each wash. The precipitates were then dried at 60 °C. Thermogravimetric analyses were conducted on a PerkinElmer Pyris 1 TGA instrument with temperature program: 25 °C (hold 1 min), ramp 10 °C min to 900 °C (hold 1 min).

X-ray data of single crystals and powders were collected using a Bruker D8 SMART APEX II CCD diffractometer with graphite monochromator and MoK α radiation (0.71073 Å) at room temperature. The structures were solved and refined in the SHELXTL program suite. All non-hydrogen atoms were found in the initial solution for both compounds. Data collected was performed at room temperature. The powder data was treated and analyzed with the Bruker APEX2 program suite and EVA v12. For details of structure refinement, please, see Table 1. The Checkcif evaluation render a number of B alerts associated with refinement of the rhombohedral structure in a hexagonal setup (so called hexagonal doubly centered) – this is a normal procedure in the SHELXTL program suite. Also, the observed R_{int} value was relatively high, 0.208, as a result of merohedral twinning distinguishable in polarized light. Major part of domains not belonging to the main orientation were removed by physical cutting-off, but the remaining minor residues resulted in elevated R_{int}, R1 and wR2 values.

FTIR spectra were collected by a PerkinElmer Spectrum-100 FTIR spectrometer. Crystals of 1 were washed several times in MilliQ-water, dried under a desktop lamp, milled in anhydrous KBr (FTIR-grade, Sigma-Aldrich, dried overnight at 200 °C) and then pressed into pellets. Spectra were collected for 4000–400 cm⁻¹ with 1 cm⁻¹ resolution and 16 scans per spectrum. All NMR spectra were recorded using a Bruker Avance 600 MHz SmartProbe spectrometer with Bruker TopSpin version 3.5. The spectra were processed and analyzed in Bruker Topspin version 3.6. The ¹H spectra were calibrated against the internal water signal from residual non-deuterated water. All spectra were recorded at 298 K. MilliQ water or 0.1 M HCl with ca. 10 v% D₂O (euriso-top, 99.96 % d) was used as solvent mixture for recording of NMR data. Scanning

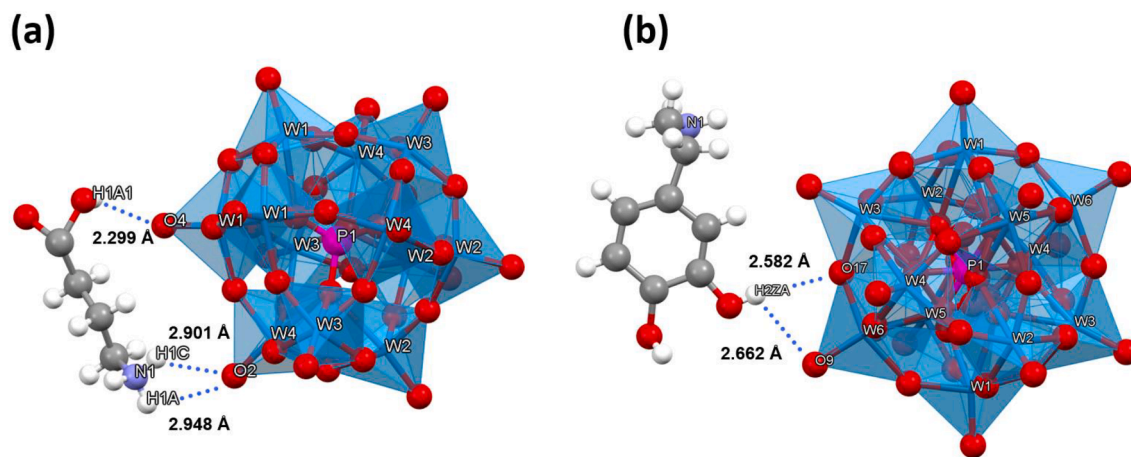


Fig. 1. (a) Molecular structure of compound 1, [(HGABA)₃PW₁₂O₄₀]. (b) Molecular structure of compound 2, [(Hdopamine)₂HPW₁₂O₄₀] [33]. Hydrogen bonds are indicated by blue dotted lines. Solvating water molecules in compound 2 have been omitted. The NH₃-group of dopamine binds an adjacent [PW₁₂O₄₀]³⁻ ion (not indicated in figure), thus acting as a connector. Blue is tungsten, magenta is phosphorous, red is oxygen, grey is carbon, light purple is nitrogen, and white is hydrogen.

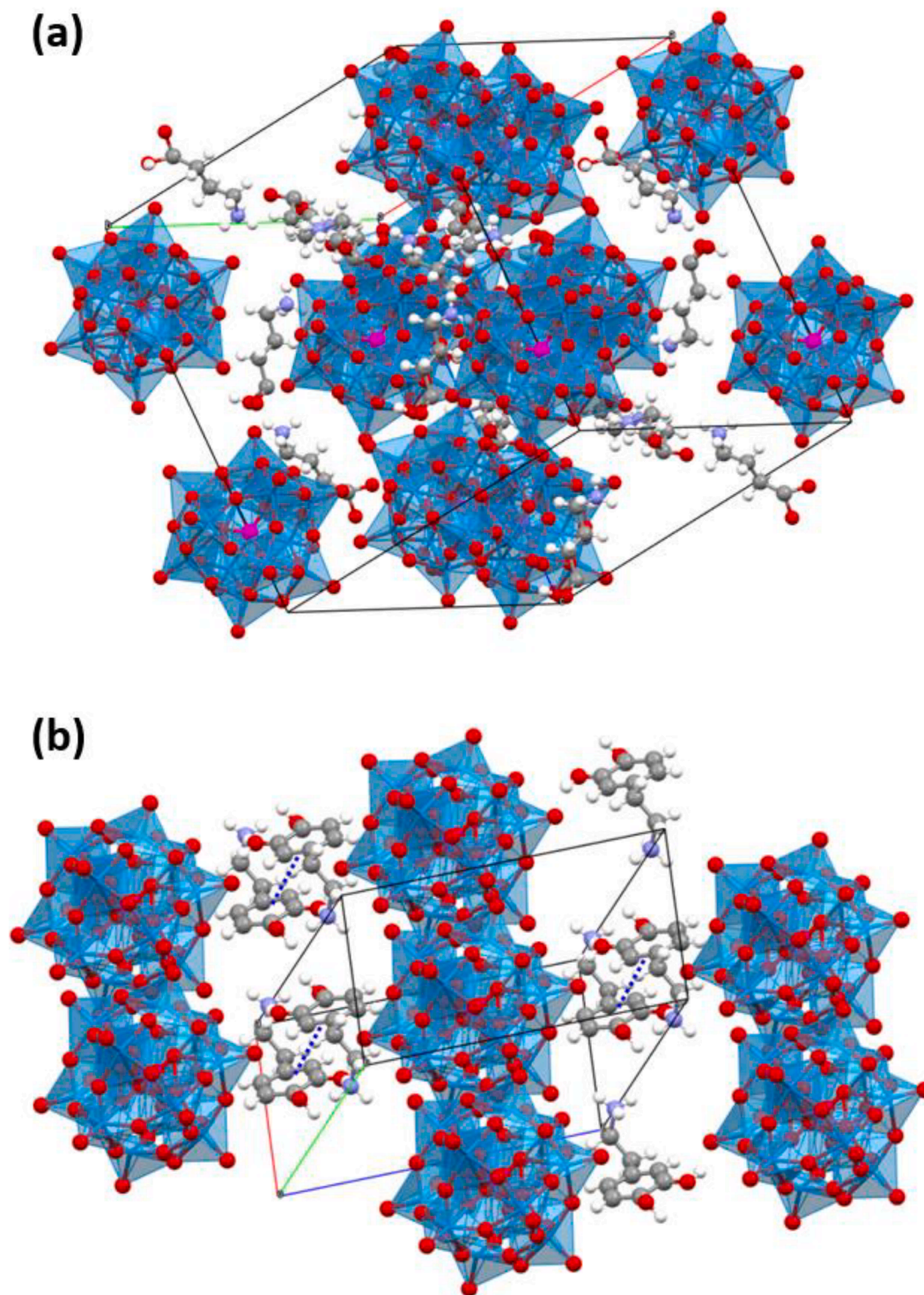


Fig. 2. Packing of (a) compound 1 and (b) compound 2. The distance between the centroids (indicated by blue dots) of the closely packed dopamine molecules is 4.473 Å. Solvating water molecules in compound 2 was removed for clarity.

electron microscopy (SEM) was performed by a Hitachi TM-1000 tabletop scanning electron microscope. Self-assembly studies were done in 100 mM phosphate buffer at pH 7, 8, or borate buffer at pH 9, using different m/m ratios of H₃PW₁₂O₄₀: ligand. In cases where precipitates were formed, these were centrifuged and washed with MilliQ-water and analyzed by SEM. TGA measurements were performed with Perkin-Elmer Pyris 1 instrument.

3. Results and discussion

Mixture of H₃PW₁₂O₄₀ with different equivalents (0.5 to 4) of GABA in various solvent systems only resulted in the crystallization of H₃PW₁₂O₄₀ as colorless, flat squares. In an attempt to facilitate the crystallization, dopamine was added in small amounts to co-crystallize GABA and dopamine with phosphotungstate. This resulted in the formation of dark red cubic crystals of compound 1, [(HGABA)₃PW₁₂O₄₀] (Fig. 1a). The previously reported [(Hdopamine)₂HPW₁₂O₄₀] complex

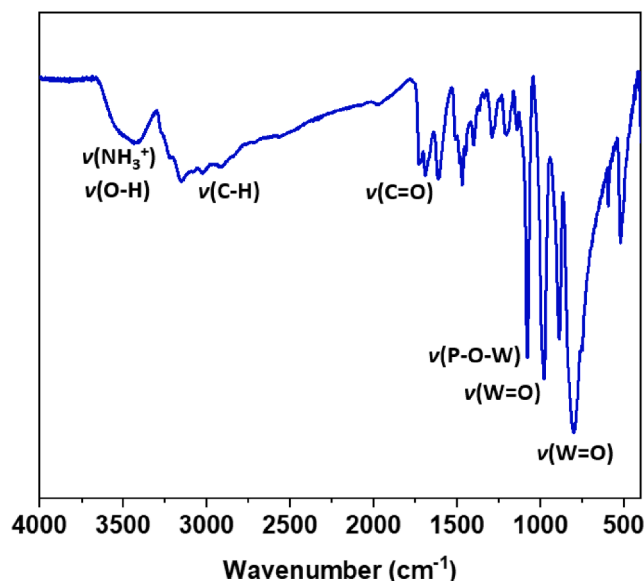


Fig. 3. FTIR of compound 1 with indicated signal interpretation.

[33], compound 2 (Fig. 1b), crystallized separately as red needles. Packing in the structures of 1 and 2 differs considerably, featuring complex aggregated layers for the former and much simpler layered structure for the latter (See Fig. 2).

The addition of one more potential ligand to promote crystallization without itself being present in the crystal structure have been reported before [34]. Compound 1 crystallized in the rhombohedral space group *R*-3. Detailed crystallographic description is provided in Table 1. Protonated HGABA unit interacts with $[PW_{12}O_{40}]^{3-}$ via very strong hydrogen bonding between the carboxylic hydroxyl group and a terminal oxygen, H1A1 – O4(W1) (2.299 Å) and two amino group's hydrogen atoms, H1C – O2(W4) (2.901 Å) and H1A – O2(W4) (2.948 Å). In the packing, GABA molecules hydrogen bond to each other via the amino group and the carbonyl oxygen (N1)H1C – O2A(C1) (2.318 Å). Notably, there are no solvating water molecules in the structure of compound 1. The aromatic rings of dopamine in compound 2 are tilted towards each other with a distance of 4.473 Å between the centroids. This distance is on the border between very weak π - π interaction and van der Waals interaction. In addition, the dopamine molecules also revealed relatively strong hydrogen bonding between their hydroxyl groups and the protonated amino group; O2Z – H1B(N1) 2.093 Å, and O3Z – H1C(N1) 2.486 Å.

3.1. Infrared spectrometry

FTIR spectra were recorded of washed and dried crystals of compound 1, (Fig. 3). Vibrations at 1080 cm^{-1} $\nu(\text{P}-\text{O}-\text{W})$, 980 cm^{-1} $\nu(\text{W}=\text{O})$, 888 cm^{-1} and 800 cm^{-1} as $\nu(\text{W}-\text{O})$ [35], 1690 cm^{-1} as $\nu(\text{C}=\text{O})$ from GABA, and weak signal at 2911 cm^{-1} as $\nu(\text{C}-\text{H})$ from GABA, a broad region between 3200 cm^{-1} to 3660 cm^{-1} are assigned to overlapping $\nu(\text{O}-\text{H})$ and $\nu(\text{NH}_3^+)$ vibrations.

3.2. Self-assembly studies

Dopamine was previously reported to guide the self-assembly of phosphotungstic acid, phosphomolybdic acid, and tungsten oxide into well-defined flower-like structures [28,31,32], but it was not until very recently a molecular model for the interaction between dopamine and POM was reported [33]. In this work, we crystallized phosphotungstate with GABA as a part of our work to better understand interactions between biologically important molecules and metal oxide nanoparticles. It was also of interest to investigate whether GABA also could direct self-assembly of POMs, and also to get a better insight the mechanism behind self-assembly with dopamine. GABA was mixed in different ratios with $\text{H}_3\text{PW}_{12}\text{O}_{40}$ (1 to 4, m/m) in 100 mM phosphate buffer, at different pH 7, 8, or 100 mM borate buffer pH 9. However, no self-assembled structures were observed. Both GABA and dopamine interact with $\text{H}_3\text{PW}_{12}\text{O}_{40}$ via hydrogen bonding with both an OH-group and a NH_3 -group. This suggest that π - π stacking between the aromatic rings may be crucial to direct the self-assembly. To further investigate the role of the amine group of dopamine, a number of other catechols, lacking the amine group, were used (See Fig. 4). Three different catechols, pyrocatechol (1,2-dihydroxybenzene, PC), 4-methylcatechol (4mC), and 4-*tert*-butyl catechol (4tBC), were mixed in different ratios (1 to 4, m/m) with $\text{H}_3\text{PW}_{12}\text{O}_{40}$ in the same phosphate buffers.

Of these three, only 4tBC managed to produce self-assembled structures, which were rather polydisperse spheres (Fig. 5), much larger (ca. 100 nm to 500 nm) than the flower-like structures using dopamine as reported by [28]. From Fig. 5d it is evident that they are built up of much smaller particles. The ratios of $\text{H}_3\text{PW}_{12}\text{O}_{40}$: 4tBC did not appear to have any major influence on the self-assembly for pH 7, but increasing the pH apparently inhibited the formation of spheres. Attempts to crystallize 4tBC with $\text{H}_3\text{PW}_{12}\text{O}_{40}$ under various conditions were unsuccessful.

3.3. Power X-ray diffraction

Powder X-ray diffraction (PXRD) was employed to investigate possible influence on the crystalline phase of the precipitated powder. From the diffractograms in Fig. 6 it is evident that different crystalline products are formed. $\text{H}_3\text{PW}_{12}\text{O}_{40}$:dopamine (1:1) resulted in a powder

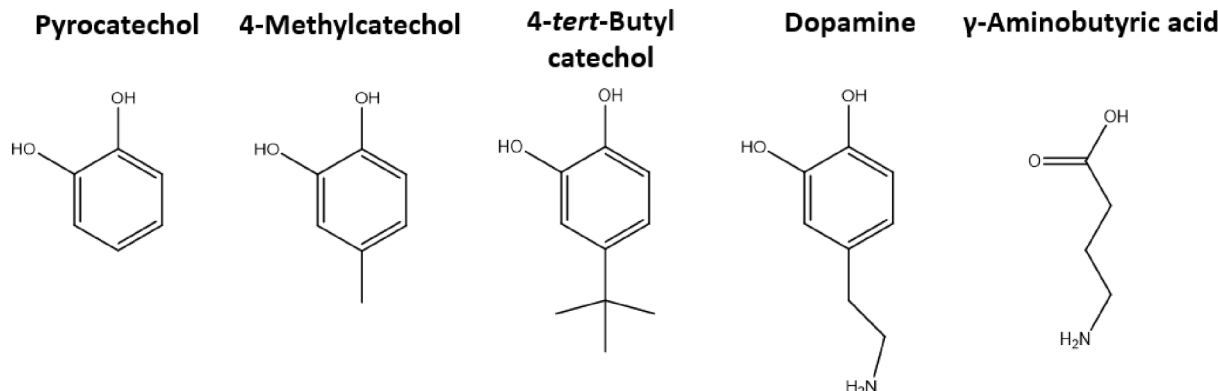


Fig. 4. Chemical structures of the four different catechols and GABA.

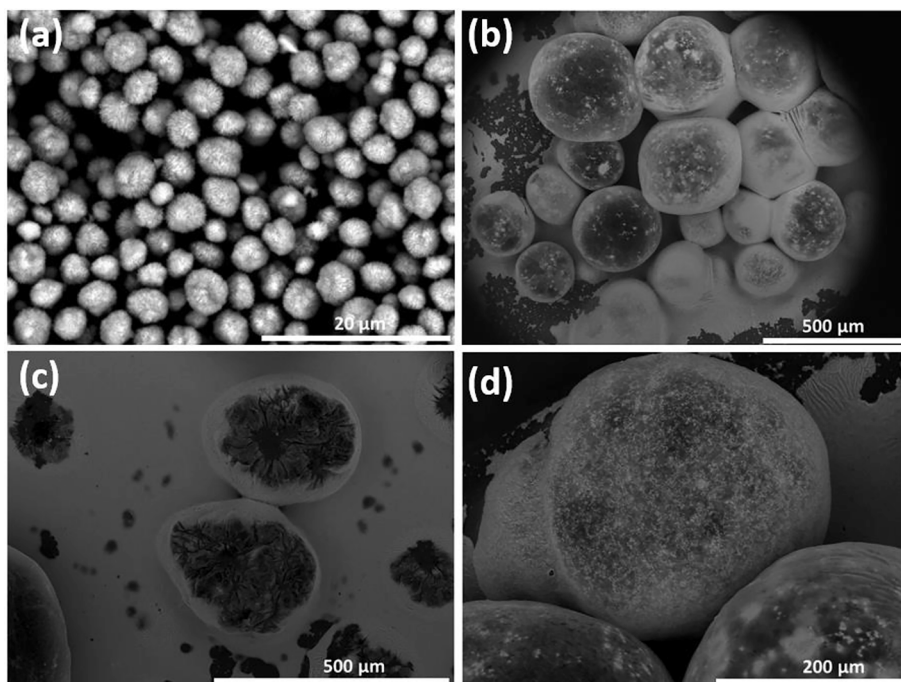


Fig. 5. SEM micrographs of self-assembled $\text{H}_3\text{PW}_{12}\text{O}_{40}$ with dopamine or GABA. (a) $\text{H}_3\text{PW}_{12}\text{O}_{40}$:dopamine 1:1 (m/m) reference as reported by Li et al., [33], here in 100 mM phosphate buffer pH 7 as solvent. (b) $\text{H}_3\text{PW}_{12}\text{O}_{40}$:4tBC 1:1 (m/m) in 100 mM phosphate buffer, pH 7. (c) Incomplete self-assembled spheres of $\text{H}_3\text{PW}_{12}\text{O}_{40}$:4tBC. (d) Magnification of a $\text{H}_3\text{PW}_{12}\text{O}_{40}$:4tBC sphere, revealing it is constructed of smaller units.

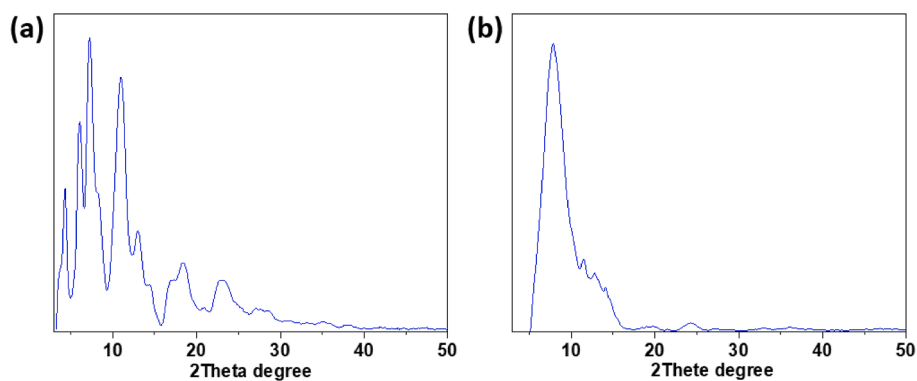


Fig. 6. PXRD patterns of precipitated (a) $\text{H}_3\text{PW}_{12}\text{O}_{40}$:dopamine (1:1) (2θ : 4.26°, 6.0°, 7.26°, 11.04°, 13.02°, 18.36°, and 23.16°) and (b) $\text{H}_3\text{PW}_{12}\text{O}_{40}$:4tBC (1:1) (2θ : 7.92°, 11.52°, 12.78°, 14.10°, and 24.42°) from Fig. 5.

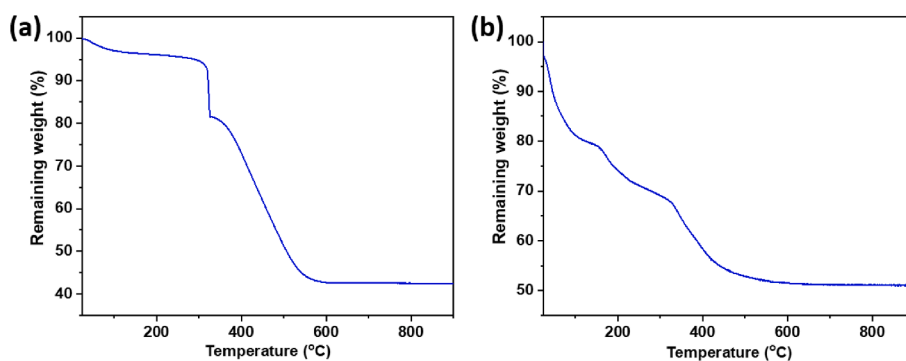


Fig. 7. Thermogravimetric analysis of precipitates of (a) $\text{H}_3\text{PW}_{12}\text{O}_{40}$:dopamine and (b) $\text{H}_3\text{PW}_{12}\text{O}_{40}$:4tBC.

of higher crystallinity compared to $\text{H}_3\text{PW}_{12}\text{O}_{40}$:4tBC (1:1). Neither diffraction pattern matched any known phases but they both appear to consist of mixtures of different tungsten oxides.

3.4. Thermogravimetric analysis

Washed precipitates of $\text{H}_3\text{PW}_{12}\text{O}_{40}$:dopamine and $\text{H}_3\text{PW}_{12}\text{O}_{40}$:4tBC

Table 2

Diffusion coefficients for dopamine and GABA in different solvents.

	MilliQ (with 10 v% D ₂ O)	0.1 M HCl (with 10 v% D ₂ O)
Dopamine	5.74·10 ⁻¹⁰ m ² s	5.54·10 ⁻¹⁰ m ² s
GABA	8.61·10 ⁻¹⁰ m ² s	8.89·10 ⁻¹⁰ m ² s
<i>In mixture</i>		
Dopamine	7.92·10 ⁻¹⁰ m ² s	5.61·10 ⁻¹⁰ m ² s
GABA	1.12·10 ⁻⁹ m ² s	8.53·10 ⁻¹⁰ m ² s

were analyzed by TGA (See Fig. 7). For H₃PW₁₂O₄₀:dopamine there is a slight weight loss starting at ca. 100 °C which may be ascribed to water, followed by a very slow weight decrease until ca. 300 °C, when dopamine starts to decompose. For H₃PW₁₂O₄₀:4tBC there is an initial fast weight decrease in two steps, from 25 °C to ca. 120 °C, and 160 °C to 300 °C, both of which may be removal of the more volatile 4tBC and residual water. The third weight decrease at ca. 320 °C would be the decomposition of more strongly bound 4tBC, which is finalized at ca. 600 °C. This indicates a stronger interaction between H₃PW₁₂O₄₀ and dopamine.

3.5. NMR spectrometry

In order to investigate potential interactions between the ligands in solution ¹H DOSY was employed to measure diffusion coefficients. ¹H DOSY spectra for dopamine and GABA were recorded individually and together in both MilliQ-water with 10 v% D₂O and 0.1 M HCl with 10 v% D₂O. The measured diffusion coefficients are reported in Table 2. Concentrations and GABA: dopamine ratios were the same as for the synthesis of compound 1. Aqueous systems were chosen to resemble the crystallization conditions. The H₃PW₁₂O₄₀:GABA-dopamine mixture was not soluble in MilliQ-water and crystallized in the NMR tube during spectra acquisition while using 0.1 M HCl, thus no satisfying DOSY spectrum was obtained. The difference in diffusion coefficients between pure solutions of dopamine and GABA did not differ very much between MilliQ-water and 0.1 M HCl, but the differences were larger for the mixture in MilliQ-water.

4. Conclusions

In this work we have reported the crystal structure of the new [(HGABA)₃PW₁₂O₄₀] complex. The interaction in solution between GABA and the POM was apparently weak as the complex would not crystallize without the addition of dopamine, i.e. the so-called “cocktail effect”. This could be of relevance for metal and metal oxide nanoparticles entering biological systems where they come in contact with complex mixtures of biomolecules, which potentially could result in enhanced interaction between certain components. The influence of dopamine on the crystallization of other systems is currently under investigation. The crystal structures of [(HGABA)₃PW₁₂O₄₀] and [(Hdopamine)₂HPW₁₂O₄₀], together with studies of catechols structurally similar to dopamine, provides a tentative molecular explanation for the well-reported structure-directing effect of dopamine where interactions between the aromatic rings are proposed to be important. This may assist identification of new structure directing ligands.

Declaration of Competing Interest

The authors declare that they have no known competing financial interests or personal relationships that could have appeared to influence the work reported in this paper.

Acknowledgements

This work was supported by the Swedish Research Council

(Vetenskapsrådet) grant number 2014-3938 and 2018-03811. The authors express their sincerest gratitude to Prof. Gulaim Seisenbaeva for the help with TGA measurements.

Appendix A. Supplementary data

Crystallographic data are available free of charge from the Cambridge Crystallographic Data Center. The CCDC reference numbers for compounds 1 and 2 are 2074443 and 2015440, respectively. Supplementary data to this article can be found online at <https://doi.org/10.1016/j.ica.2021.120547>.

References

- [1] V. Bhardwaj, A. Kaushik, *Micromachines* 8 (2017) 10.
- [2] C.L. Wang, X.M. Li, F. Zhang, *Analyst* 141 (2016) 3601–3620.
- [3] P. Vega-Vasquez, N.S. Mosier, J. Irudayaraj, *Front. Bioeng. Biotech.* 8 (2020) 79.
- [4] O.S. Wolfbeis, *Chem. Soc. Rev.* 44 (2015) 4743–4768.
- [5] R.Z. Liang, M. Wei, D.G. Evans, X. Duan, *Chem. Comm.* 50 (2014) 14071–14081.
- [6] O.L. Evdokimova, F.G. Svensson, A.V. Agafonov, S. Hakansson, G.A. Seisenbaeva, V.G. Kessler, *Nanomaterials* 8 (2018) 228.
- [7] G.A. Seisenbaeva, K. Fromell, V.V. Vinogradov, A.N. Terekhov, A.V. Pakhomov, B. Nilsson, K.N. Ekdahl, V.V. Vinogradov, V.G. Kessler, *Sci. Rep.* 7 (2017) 15448.
- [8] J. Tian, K.K.Y. Wong, C.M. Ho, C.N. Lok, W.Y. Yu, C.M. Che, J.F. Chiu, P.K.H. Tam, *ChemMedChem* 2 (2007) 129–136.
- [9] A. Servin, W. Elmer, A. Mukherjee, R. de la Torre-Roche, H. Hamdi, J.C. White, P. Bindraban, C. Dimkpa, *J. Nanopart. Res.* 17 (2015) 92.
- [10] B. Fadeel, *Front. Immunol.* 10 (2019) 133.
- [11] E. Kranjc, D. Drobne, *Nanomaterial* 9 (2019) 1094.
- [12] J.T. Rhule, C.L. Hill, D.A. Judd, *Chem. Rev.* 98 (1998) 327–357.
- [13] C.K. Perkins, E.S. Eitheim, B.L. Fulton, L.B. Fullmer, C.A. Colla, D.H. Park, A. F. Oliveri, J.E. Hutchison, M. Nyman, W.H. Casey, T.Z. Forbes, D.W. Johnson, D. A. Keszler, *Angew. Chem. Int. Ed.* 56 (2017) 10161–10164.
- [14] M.R. Horn, A. Singh, S. Alomari, S. Goberna-Ferrón, R. Benages-Vilau, N. Chodankar, N. Motta, K. Ostrikov, J. MacLeod, P. Sonar, P. Gomez-Romero, D. Dubal, *Energy Environ. Sci.* 14 (2021) 1652–1700.
- [15] E. Tanuhadi, I. Kampatsikas, G. Giester, A. Rompel, *Monatsh. Chem.* 150 (2019) 871–875.
- [16] E. Tanuhadi, N.I. Gumerova, A. Prado-Roller, M. Galanski, H. Cipicic-Paljetak, D. Verbanac, A. Rompel, *Inorg. Chem.* 60 (2021) 28–31.
- [17] E. Nikoloudakis, K. Karikis, M. Laurans, C. Kokotidou, A. Solé-Daura, J.J. Carbó, A. Charalambidis, G. Charalambidis, G. Izzet, A. Mitraki, A.M. Douvas, J.M. Poblet, A. Proust, A.G. Coutsolelos, *Dalton Trans.* 47 (2018) 6304–6313.
- [18] T. Minato, K. Suzuki, K. Yamaguchi, N. Mizuno, *Chem. Eur. J.* 53 (2017) 14213–14220.
- [19] A.V. Anyushin, S. Vanhaecht, T.N. Parac-Vogt, *Inorg. Chem.* 59 (2020) 10146–10152.
- [20] T.T. Mihaylov, H.G.T. Ly, K. Pierloot, T.N. Parac-Vogt, *Inorg. Chem.* 55 (2016) 9316–9328.
- [21] H.G.T. Ly, G. Absillis, S.R. Bajpe, J.A. Martens, T.N. Parac-Vogt, *Eur. J. Inorg. Chem.* 26 (2013) 4601–4611.
- [22] L. Vandebroek, Y. Mampaey, S. Antonyuk, L. van Meerelt, T.N. Parac-Vogt, *Eur. J. Inorg. Chem.* 3–4 (2019) 506–511.
- [23] B. Greijer, T. de Donder, G. Nestor, J.E. Eriksson, G.A. Seisenbaeva, V.G. Kessler, *Eur. J. Inorg. Chem.* 1 (2021) 54–61.
- [24] A. Bijelic, M. Aureliano, A. Rompel, *Chem. Comm.* 54 (2018) 1153–1169.
- [25] H. Yanagie, A. Ogata, S. Mitsui, T. Hisa, T. Yamase, M. Eriguchi, *Biomed. Pharmacother.* 60 (2006) 349–352.
- [26] F.G. Svensson, G.A. Seisenbaeva, N.A. Kotov, V.G. Kessler, *Materials* 13 (2020) 4856.
- [27] K. Okumura, S. Ishida, R. Takahata, N. Katada, *Catal. Today* 204 (2013) 197–203.
- [28] H. Li, Y. Jia, A.H. Wang, W. Cui, H.C. Ma, X.Y. Feng, J. Li, *Chem. Eur. J.* 20 (2014) 499–504.
- [29] G.A. Seisenbaeva, M.P. Moloney, R. Tekoriute, A. Hardy-Dessources, J.M. Nedelec, Y.K. Gunko, V.G. Kessler, *Langmuir* 26 (2010) 9809–9817.
- [30] H. Zhang, L.Y. Guo, J.M. Jiao, X. Xin, D. Sun, S.L. Yuan, *ACS Sustain. Chem. Eng.* 5 (2017) 1358–1367.
- [31] H. Li, Y.Y. Zhao, C. Yin, L. Jiao, L.Q. Ding, *Colloid. Surface A.* 572 (2019) 147–151.
- [32] L.S. Sun, Y. Qi, C.L. Wang, M.L. Guan, J.X. Qiu, B.B. Tian, H.M. Li, L. Wang, *ACS Sustain. Chem. Eng.* 8 (2020) 18966–18974.
- [33] F.G. Svensson, V.G. Kessler, *J. Mol. Struct.* 1226 (2021), 129343.
- [34] A.K. Adcock, R.L. Ayscue, L.M. Breuer, C.P. Verwiel, A.C. Marwitz, J.A. Bertke, V. Vallet, F. Real, K.E. Knope, *Dalton Trans.* 49 (2020) 11756–11771.
- [35] K.M. Rominger, G. Nestor, J.E. Eriksson, G.A. Seisenbaeva, V.G. Kessler, *Eur. J. Inorg. Chem.* (2019) 4297–4305.